J Appl Electrochem (2008) 38:1749–1755
DOI 10.1007/s10800-008-9626-z

ORIGINAL PAPER

Enhanced degradation of aqueous methyl orange by contact glow discharge electrolysis using Fe^{2+} as catalyst

Jianying Gong · Juan Wang · Weijie Xie · Weimin Cai

Received: 19 November 2007 / Accepted: 25 June 2008 / Published online: 19 July 2008

Abstract The enhanced degradation of methyl orange in aqueous solution was achieved by means of contact glow discharge electrolysis (CGDE) through adding a small amount of Fe^{2+} to the solution. Methyl orange was degraded and eventually decomposed into inorganic carbon when CGDE was carried out under an applied DC voltage of 480 V and a current of 65–80 mA. The oxidation process followed first-order kinetics; the degradation rate increased almost eight times in the presence of Fe^{2+}. A reaction pathway is proposed based on analysis of the ultraviolet (UV) spectra of the solution and intermediate products from High Performance Liquid Chromatography-Mass Spectrometry (HPLC-MS). The addition of hydroxyl radicals promoted by the Fe^{2+} catalyst is a key step in enhancing the whole oxidation process.

Keywords Contact glow discharge · Plasma · Degradation · Methyl orange · Fenton's reaction

1 Introduction

Water pollution caused by dyes has become a serious problem in developing countries. Dyes are used by many industries to color their products. The discharge of dye-containing wastewater not only causes eutrophication of receiving water bodies but incorporates the bio-refractory components as well, adding to the difficulty of treating and purifying the wastewater [1–3]. Contact glow discharge electrolysis (CGDE) is a technology that has been systematically studied since the 1960s [4]. In CGDE, plasma is generated locally between a platinum wire anode electrode and the surface of a liquid solution when the applied voltage is increased to a threshold value, normally 0.42 kV [4, 5]. The most distinct feature of CGDE is its non-faradaic chemical effects [6–10]: the yields obtained at the glow-discharge electrode are several times the faradaic value and the products are unique compared with conventional electrolysis. In the reaction zone, within the plasma at the anode, vapor phase H_2O water molecules are ionized and activated, resulting in ion bombardment and hemolytic fission. Free OH and H radicals [11] are produced through energy transfer. At the same time, in the liquid-phase reaction zone near the plasma–anolyte interface, liquid phase H_2O molecules are dissociated into H_2, H_2O_2 and O_2 as a result of bombardment by highly energized $H_2O_{gas}{}^+$ from the anodic plasma [10]. A mixture of the active species $OH^\bullet$, $H^\bullet$ and $H_2O_{gas}{}^+$ diffuse across the primary zone (called the plasma layer) into the bulk electrolyte. These species are strong oxidizing agents. Thus, CGDE can be used in advanced oxidation processes (processes which are based on the generation of radical intermediates [12]). CGDE has been used for wastewater treatment by degradation of phenol [13], chlorophenols [14], 2,4-dichlorophenol [15], benzoic acid [16], aniline [17] and alkylbenzenesulfonates [18]. Gao et al have used this method to treat dyes such as acridine orange (OA) [19], α-naphthol [20], red B and flavine G [21]. Recently, we have applied the CGDE method to degrade methyl orange (MO). The degradation kinetics and mechanism were studied. However, the degradation rate was low (nearly 48.8% for 90 min) [22].

It is well known that the ferrous ion can react with hydrogen peroxide to produce hydroxyl radicals which can be used to oxidize organic pollutants. In this work, the

J. Gong · J. Wang · W. Xie · W. Cai (✉)
School of Environmental Science and Engineering, Shanghai Jiaotong University, Shanghai 200240, China
e-mail: gjy@sjtu.edu.cn

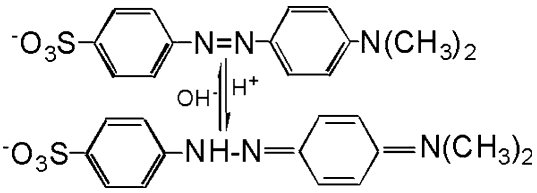

Scheme 1 The structure of MO

catalytic effect of the ferrous ion on the degradation of MO using CGDE has been studied. To our knowledge there are no reported data on the degradation of MO using CGDE with Fe^{2+} as catalyst. The structures of MO in acidic and basic solution are shown in Scheme 1.

2 Experimental

The apparatus is illustrated in Fig. 1. The reaction vessel was made up using two cylindered glass tubes (4 cm diameter) connected by a sintered glass disk with medium porosity at the bottom. The anode consisted of a platinum wire (0.5 mm diameter) held in a brass support. The cathode was a stainless steel plate (4 cm^2 in area) placed in another glass tube. Both the anode and the cathode were immersed into the solution during the reaction. During degradation argon gas was passed through the solution to remove air. The anode was immersed into the solution to a depth of approximately 2 mm. The power supply was a DH1722-6 direct current power unit which provided voltages of 0–1000 V and a maximum output of 300 mA. The

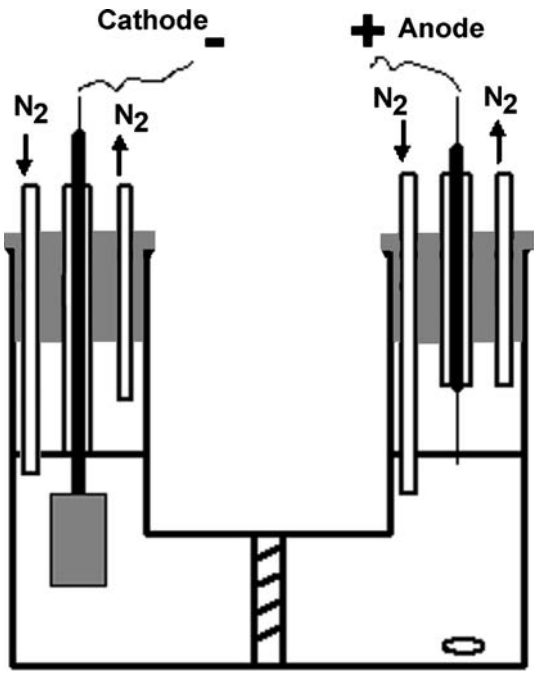

Fig. 1 Sketch of CGDE reaction apparatus

Table 1 Experimental conditions

Parameter	Value
Voltage range (V)	480
The range of current (mA)	65–80
Distance between electrodes (mm)	40
Diameter of discharge electrode (mm)	0.5
Aqueous Na_2SO_4 (M)	0.015
Methyl orange (mg/L)	4.15
pH range	2.0–3.0
Volume (mL)	200

experiments are performed under the conditions listed in Table 1 unless otherwise stated. Considerable heat was produced in the discharge during the reaction therefore the cell was placed in an ice-water bath to ensure a long-time reaction.

The solution most frequently used was 200 mL with varying concentrations of MO dissolved in sodium sulfate (0.015 M). Before each run, 1 mL of 2×10^{-3} M Fe^{2+} was added to the solution and a magnetic stir bar was used at the bottom of the anodic side of the vessel to ensure that the solution mixed well. The concentration of the reactant obtained was determined by a UNICO UV-2102 spectrophotometer. The solution pH was measured using an REX PHSJ-3F pH meter. At the end of the reaction the products in solution, as well as starting materials, were analyzed by means of high performance liquid chromatography-mass spectroscopy (HPLC-MS) HP1100LC-MS (Agilent Integrity System).

HPLC conditions included a C_{18} 4-μm column (4.6×150 mm) used for separations. The mobile phase was a mixture of 80% solvent A (methanol) and 20% solvent B (H_2O). The flow rate was 0.7 mL min^{-1}. The detector wavelength was 220 nm. The injection volume was 5 μL. For mass spectrometric analysis, electrospray ionization (ESI) mass spectra were obtained. The mass spectrometer was operated in positive ion mode. The detailed conditions of MS were as follows: capillary voltage was 3,500 V, nebulizer pressure was 25 psi and the skimmer was 70 V. The flow rate of the drying gas was 9 L min^{-1} and the temperature of the drying gas was maintained at 350 °C.

3 Results and discussion

3.1 Relationship of current and voltage during the course of reaction

Figure 2 shows the different current (I) and voltage (U) values during the electrolysis reaction to attain CGDE in the presence of Fe^{2+}. When the voltage changed from 0 to

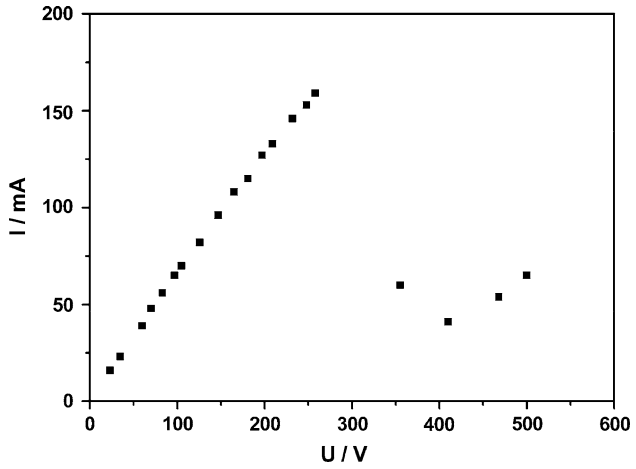

Fig. 2 Current–voltage graph

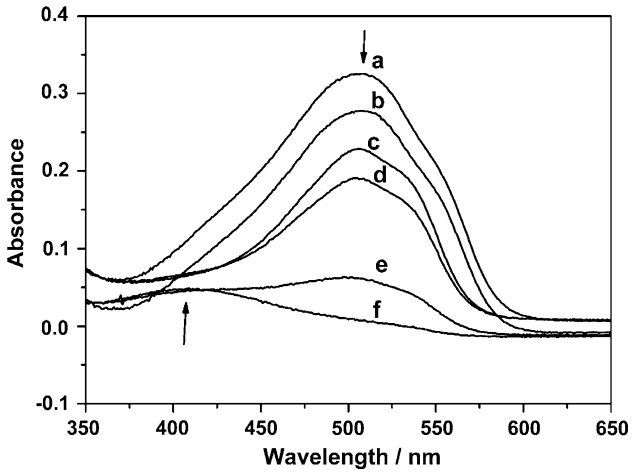

Fig. 3 UV absorption spectra of (a) untreated MO solution (b) 5 min (c) 10 min (d) 20 min (e) 30 min (f) 40 min in the presence of 2×10^{-3} M Fe^{2+} at different degradation time under CGDE

260 V, the current value changed correspondingly from 0 to 160 mA The relationship between I and U obeys Ohm's law. Small bubbles produced from the pointed side of the anode were observed. When the applied voltage was higher than 420 V, the current fell to its lowest value indicating a turning point in the whole change of *I* and *U*. During the reaction, keeping the U value above 260 V for a few minutes, the voltage value began increasing abruptly from 260 to 300 V and then kept rising to 420 V where the current fell quickly to its lowest point at 40 mA. Simultaneously, a weak glow spot on the pointed side of the anode appeared. Adjusting the voltage to 480 and 500 V caused an increase in current and a brightening of the glow spot with sparks was observed. Its normal size was less than 1 cm^2 from the anode across the anolyte. In comparison to the work of Hickling and Ingram [4] and Sengupta [10], it is clear that the reaction is significantly enhanced under CGDE.

The UV absorption spectra of MO in the presence of 2×10^{-3} M Fe^{2+} at different degradation times are shown in Fig. 3. Before the reaction, the absorption curve had maximum absorption at 507 nm. Lowering of the peak at 507 nm was observed with increased reaction time. Meanwhile, there was absorption at about 420 nm after half an hour's degradation. The peak at 420 nm may be attributed to N,N dimethyl-4-nitroaniline, which is an intermediate of MO degradation [23].

3.2 Degradation rate changes for MO with and without addition of Fe^{2+}

For these studies the electrolytes were prepared at a MO concentration of 4.15 mg L^{-1} in the presence of 2×10^{-3} M Fe^{2+} and in the absence of Fe^{2+}. Each of the above solutions was treated under CGDE conditions. The change in MO concentration was determined by monitoring the UV absorption peak at 507 nm at different reaction times.

The degradation behavior of MO (4.15 mg L^{-1}) with and without Fe^{2+} ions at an initial pH of 3 at different reaction times is shown in Fig. 4. For the solution in the absence of Fe^{2+} ions, the concentration of MO (Fig. 4a) decreases gradually. The longer the reaction time the more MO is degraded. The degradation of MO (Fig. 4b) is only 27.7% for MO solution over the course of 40 min. However, for the solution in the presence of Fe^{2+} ions, the concentration of MO decreases much faster. The degradation is nearly 91.6% for MO aqueous solution in the presence of Fe^{2+} over 40 min.

3.3 Dynamic behavior analysis

The data of Fig. 4 was fitted to the following equation:

$$\ln(c_0/c_t) = kt$$

where c_0 is the initial concentration of MO, c_t is the concentration of MO at reaction time *t*, *k* is the first order rate constant in min^{-1} and *t* is the time in minutes. In the absence of Fe^{2+} ions a linear relationship with correlation coefficient $R_a^2 = 0.9981$ was obtained. In the presence of Fe^{2+} ions a linear relationship with correlation coefficient $R_a^2 = 0.994$ was obtained. From Fig. 5 it is clear that MO degradation follows pseudo-first order kinetics with or without Fe^{2+} ions in solution. However, the first-order rate constant corresponding to MO solution in the presence of Fe^{2+} ions is almost eight times larger than that in the absence of Fe^{2+} ions.

3.4 pH changes

pH changes after each degradation are shown in Fig. 6. A decrease of nearly one pH unit was observed after

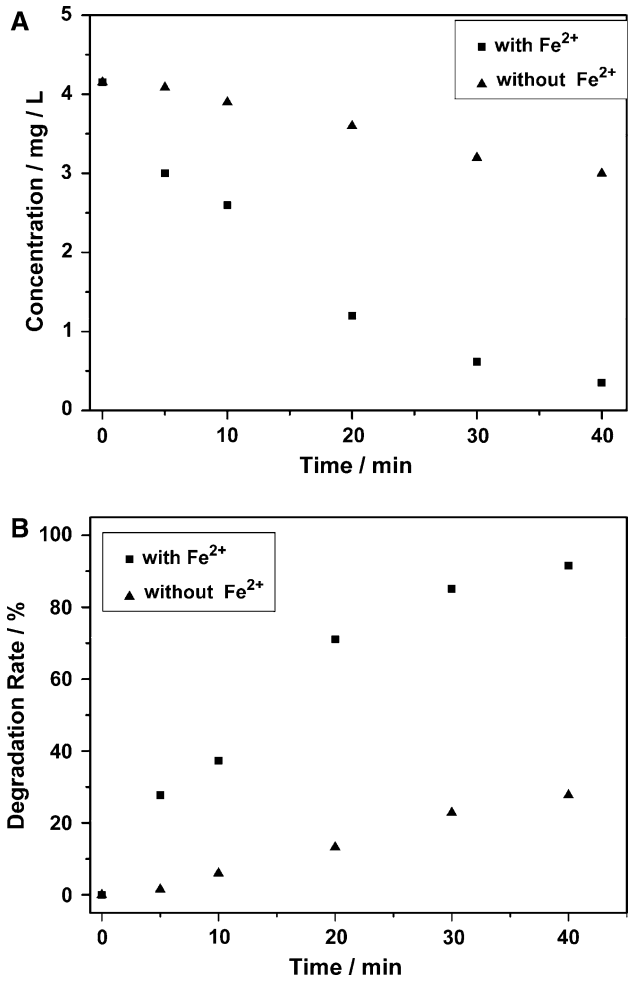

Fig. 4 CGDE oxidation of (**a**) concentration changes versus time, (**b**) degradation rate changes of MO versus time, with and without addition of Fe^{2+} ions

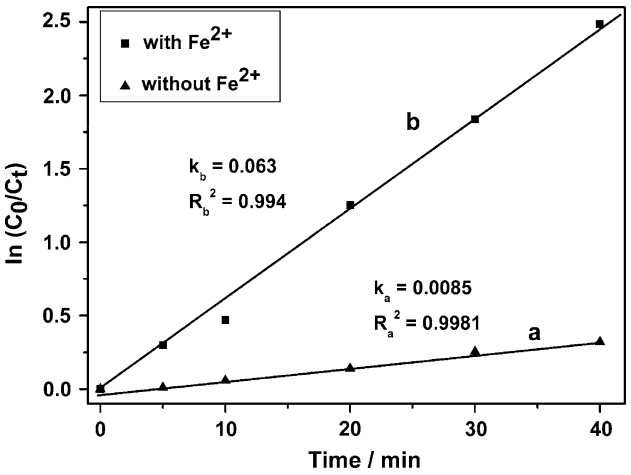

Fig. 5 Plot of dynamic analysis of degradation of MO

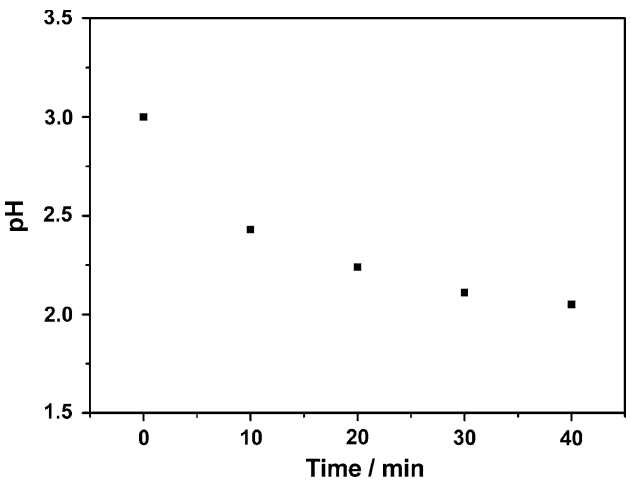

Fig. 6 Change of pH versus time

degradation. The decrease in pH can be attributed to acidic intermediates produced during the reaction which is in agreement with the presence of organic acids as stable products.

3.5 Mechanism analysis

Previous investigations of the reaction mechanism of CGDE [5–10] propose that charged species in the plasma (present in the discharge gap or sheath of vapor around the anode) are accelerated due to the steep potential gradient and enter the air–liquid interface with an energy that may be greater than 100 eV [8]. In the reaction zone, within the plasma, around the anode, vapor H_2O molecules are ionized or activated. They are bombarded by each other and broken up by an energy transfer mechanism, which results in free $^{\bullet}OH$ and $^{\bullet}H$ radicals [11], and additional non-faradaic yields of H_2 and O_2[10]. In the liquid-phase reaction zone near the plasma-anolyte interface, several liquid H_2O molecules are broken up into H_2 and H_2O_2. Additionally, O_2 that is bombarded by $H_2O_{gas}{}^+$ can diffuse across the bulk electrolyte and interact with itself or any active substrate in the solution. The overall reaction is as follows [5, 10]:

$$H_2O_{gas}{}^+ + nH_2O \rightarrow nOH^{\bullet} + nH^{\bullet} \quad (1)$$

$$H^{\bullet} + H^{\bullet} \rightarrow H_2 \quad (2)$$

$$H^{\bullet} + {}^{\bullet}OH \rightarrow H_2O \quad (3)$$

$${}^{\bullet}OH + {}^{\bullet}OH \rightarrow H_2O_2 \quad (4)$$

$${}^{\bullet}OH + H_2O_2 \rightarrow HO_2{}^{\bullet} + H_2O \quad (5)$$

Followed by [7, 10]

$$H_2O_{gas}{}^+ + H_2O \rightarrow H_2O + H_2O^+ \rightarrow {}^{\bullet}OH + H_3O^+ \quad (6)$$

$${}^{\bullet}OH + OH^{\bullet} \rightarrow H_2O + {}^1/_2O_2 \quad (7)$$

In the presence of ferrous iron the degradation of methyl orange is accelerated as shown above. Fe^{2+} reacts with

hydrogen peroxide in the CGDE process acting as a Fenton—like reagent. The oxidation process is represented by the following reactions:

$$Fe^{2+} + H_2O_2 \longrightarrow {}^{\bullet}OH + OH^- + Fe^{3+} \quad (8)$$

The ferrous iron initiates and catalyses the decomposition of hydrogen peroxide, resulting in the generation of hydroxyl radicals. The generation of the radicals involves a complex reaction sequence in aqueous solution [12].

$$Fe^{2+} + H_2O_2 \longrightarrow OH^- + OH^{\bullet} + Fe^{3+} \quad \text{(chain initiation)} \quad (9)$$

$$Fe^{2+} + {}^{\bullet}OH \longrightarrow OH^- + Fe^{3+} \quad \text{(chain termination)} \quad (10)$$

Moreover, the newly yielded ferric ions may catalyse the decomposition of hydrogen peroxide into water and oxygen [12]. The reactions are shown in Eqs. 11–14

$$Fe^{3+} + H_2O_2 \longrightarrow H^+ + FeOOH^{2+} \quad (11)$$

$$FeOOH^{2+} \longrightarrow HO_2^{\bullet} + Fe^{2+} \quad (12)$$

$$HO_2^{\bullet} + Fe^{2+} \longrightarrow Fe^{3+} + HO_2^- \quad (13)$$

$$Fe^{3+} + HO_2^{\bullet} \longrightarrow Fe^{2+} + O_2 + H^+ \quad (14)$$

Hydroxyl radicals can also oxidize organic compounds (RH) by abstraction of protons producing organic radicals ($R^{\cdot}$), which are highly reactive and can be further oxidized [24],

$$RH + {}^{\bullet}OH \longrightarrow H_2O + R^{\bullet} \quad (15)$$

The $R^{\bullet}$ may be oxidized by Fe^{3+} according to the following reactions [25],

$$R^{\bullet} + Fe^{3+} - \text{oxidation} \longrightarrow R^+ + Fe^{2+} \quad (16)$$

From the above analysis, more ${}^{\bullet}OH$ free radicals and Fe^{3+} are produced in the presence of Fe^{2+} and accelerate the degradation reaction.

3.6 Intermediate products analysis

The HPLC-MS results of the anolyte of MO, whose initial concentration is 4.15 mg L^{-1} after a reaction time of 40 min are shown in Figs. 7 and 8 respectively.

Based on the MS results of Fig. 8, the main reaction products in aqueous solution (pH = 3.0) in the presence of 2×10^{-3} M Fe^{2+}during CGDE were determined. A mechanistic scheme is presented in Fig. 9 which illustrates the reaction intermediate products and pathways of MO in aqueous solution (pH = 3.0). Figure 9 shows that the intermediate product of MO is N, N dimethyl-4-nitroaniline (m/z = 168.1), which is consistent with the results of the UV–vis spectra.

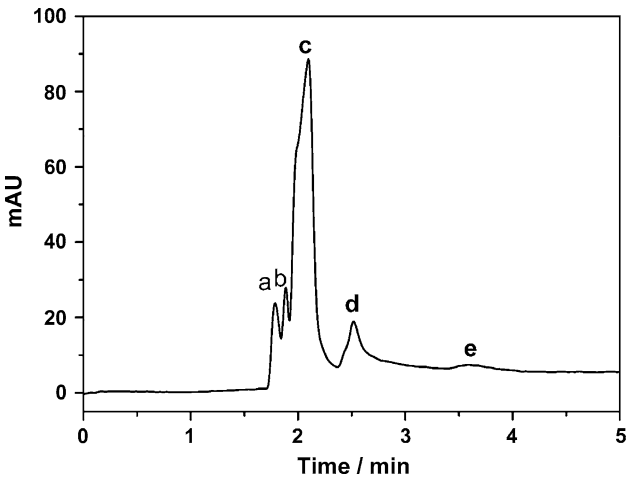

Fig. 7 HPLC plot of MO and its oxidation reaction products of CGDE

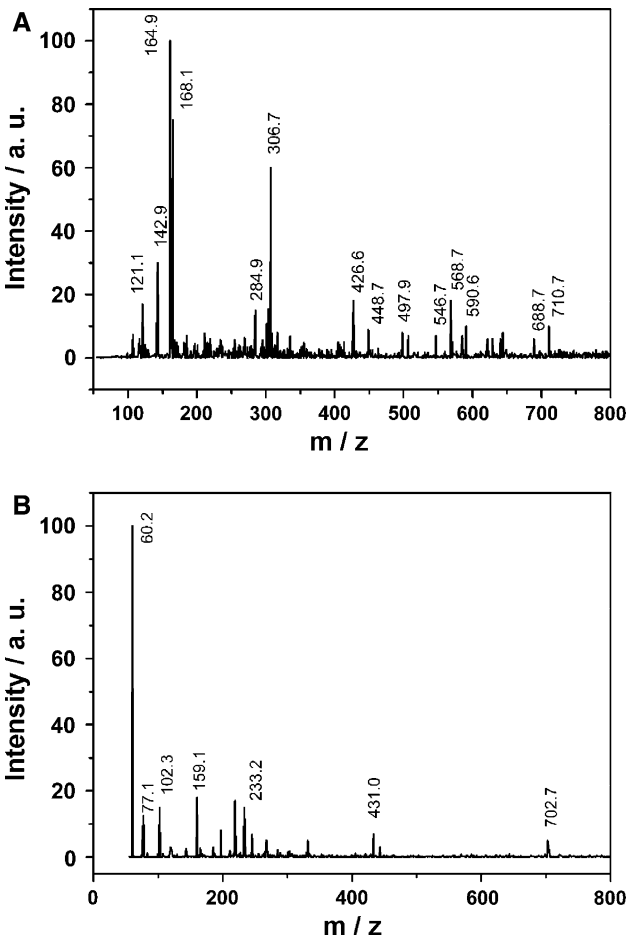

Fig. 8 MS plots of MO and its oxidation reaction products of CGDE which (**a**) comes from peak c of HPLC trace (**b**) comes from peak d of HPLC trace

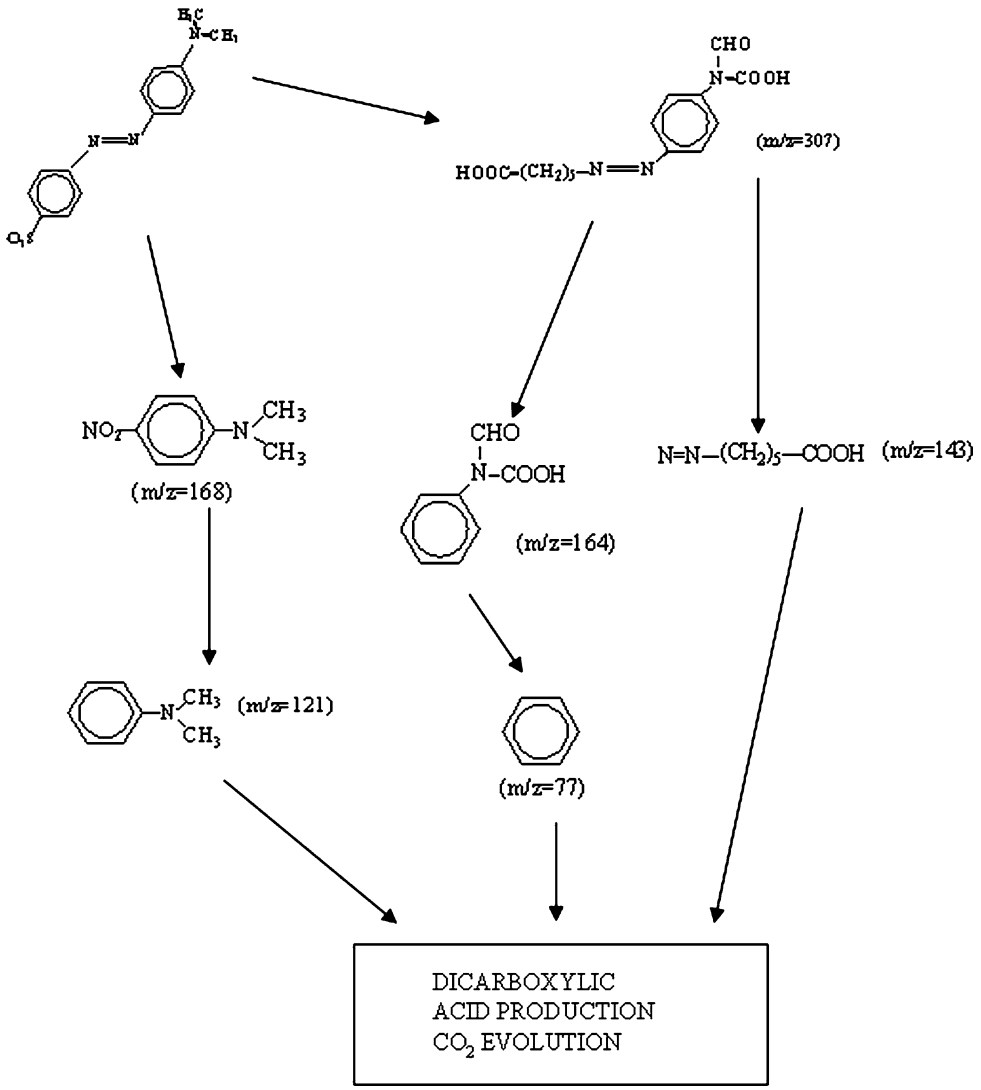

Fig. 9 Reaction products of MO in aqueous solution (pH = 3)

4 Conclusion

The enhanced degradation of MO in aqueous solution was achieved using CGDE through the addition of Fe^{2+} to the solution. The methyl orange was degraded and eventually decomposed into inorganic carbon. The oxidation process followed first-order kinetics and the degradation rate increased eight fold in the presence of Fe^{2+} compared with the absence of Fe^{2+}. The increase in hydroxyl radicals produced by the catalysis of Fe^{2+} was considered to be the key step in the oxidation enhancement. The process may be applicable in practical dye pollutant treatment.

Acknowledgements This work was supported by the Doctoral Degree Science Research Foundation from the Ministry of Education,China (No.20050248015). The authors are grateful to Elizabeth Whitsitt and Jonathan Brege of Rice University, Houston Texas for proofreading and language help.

References

1. Konstantinou IK, Albanis TA (2004) Appl Catal B-Env 49:1
2. Georgiou D, Melidis P, Aivasidis A, Gimouhopoulos K (2002) Dyes Pigments 52:69
3. Chacon JM, Leal MT, Sanchez M, Bandala ER (2006) Dyes Pigments 69:144–150
4. Hickling A, Ingram MD (1964) Trans Faraday Soc 60:783
5. Hickling A (1971) Mod Aspects Electrochem 6:329
6. Sengupta SK, Singh OP (1991) J Electroanal Chem 301:189
7. Sengupta SK, Singh OP (1994) J Electroanal Chem 369:113
8. Sengupta SK, Singh R, Srivastava AK (1998) Indian J Chem Sect A 37:558
9. Sengupta SK, Singh R, Srivastava AK (1995) Indian J Chem Sect A 34:459
10. Sengupta SK, Singh R, Srivastava AK (1998) J Electrochem Soc 145:2209
11. Bullock AT, Gavin DL, Ingram MD (1980) J Chem Soc Faraday Trans I 76:648
12. Neyens E, Baeyens J (2003) J Hazard Mater B 98:33
13. Amano R, Tomizawa S, Tezuka M (2004) Electrochem 72:836

14. Tezuka M, Iwasaki M (1998) Thin Solid Films 316:123
15. Lu QF, Yu J, Gao JZ (2006) J Hazard Mater 136:526
16. Ogata A, Miyamae K, Mizuno K, Kushiyama S, Tezuka M (2002) Plasma Chem Plasma Process 22:537
17. Tezuka M, Iwasaki M (2001) Thin Solid Films 386:204
18. Tezuka M, Amano R (2006) Water Res 40:1857
19. Gao JZ, Hu ZG, Wang XY, Hou JG, Lu XQ, Kang JW (2001) Thin Solid Films 390:154
20. Gao JZ, Pu LM, Yang W, Yu J, Li Y (2004) Plasma Process Polym 1:171
21. Gao JZ, Wang XY, Hu ZG, Deng HL, Hou JG, Lu XQ, Kang JW (2003) Water Res 37:267
22. Gong JY, Cai WM (2007) Plasma Sci Technol 9:190
23. Moussa D, Doubla A, Georges KY, Brisset JL (2007) IEEE Trans Plasma Sci 35:444
24. Walling C (1975) Acc Chem Res 8:125
25. Tang WZ, Tassos S (1997) Water Res 31:1117